

Thermal buckling of AL/AL₂O₃ functionally graded plates based on first order theory

Abdelkader FEKRAR^a, Mohamed ZIDI^a, Lakhdar BOUMIA^b, Hassen AIT ATMANE^{a,c},
Abdelouahed TOUNSI^a and El Abbas Bedia Adda^a

^a Laboratoire des Matériaux et Hydrologie, Université de Sidi Bel Abbès, BP 89 Cité Ben M'hidi 22000 Sidi Bel Abbès, Algérie.

^b Université de Sidi Bel Abbès, Département de physique, BP 89 Cité Ben M'hidi, 22000 Sidi Bel Abbès, Algérie

^c Département de Génie civil, Faculté de Génie-Civil et d'Architecture, Université Hassiba Benbouali de Chlef, Algérie

Abstract

Thermal buckling analysis of rectangular sigmoid functionally graded plates (S-FGPs) is investigated using first-order shear deformation theory. The sigmoid functionally graded material (S-FGM) system consists of ceramic (Al₂O₃) and metal (Al) phases varying through the thickness of plate according to a two power-law distribution. Material properties and thermal expansion coefficient of the plate are assumed to be graded in the thickness direction according to a simple power-law distribution in terms of the volume fractions of the constituents. The thermal loads are assumed to be uniform and sinusoidal distribution through-the-thickness. Numerical examples cover the effects of the gradient index, plate aspect ratio, side-to-thickness ratio and loading type on the critical buckling for S-FGM plates.

Keywords: S-FGM plate; Al/Al₂O₃; Buckling; Material gradient index.

1. Introduction

Functionally graded materials (FGMs) are special composites whose material properties vary continuously through their thickness. FGMs are usually made of mixture of ceramic and metal, and can thus resist high-temperature environments while maintaining toughness. The technology of FGMs was an original material fabrication technology proposed in Japan in 1984 by Sendai Group. FGMs are used in very different applications, such as reactor vessels, fusion energy devices, biomedical sectors, aircrafts, space vehicles, defense industries and other engineering structures. With the increased use of these materials for structural components in many engineering applications, the study of static, dynamic and stability behaviors of these components gains importance among researchers [1–8]. Sallai et al. [1] investigated the static responses of a sigmoid FGM thick beam by using different beam theories. Merdaci et al. [2] developed two refined displacement models for a bending analysis of functionally graded sandwich plates and the number of unknown functions involved is only four, as against five in case of other shear deformation theories. Mechab et al. [3] proposed the two variable refined plate theory. In this paper, equilibrium and stability equations of a rectangular plate made of sigmoid

functionally graded materials under thermal loads are derived based on the first order shear deformation theory. The S-FGM system consists of ceramic (Al₂O₃) and metal (Al) phases varying through the thickness of plate, according to the volume fraction of the constituent materials based on the sigmoid functions. The thermal loads are assumed to be uniform and sinusoidal temperature rises across the thickness direction are analyzed. The influence of aspect and thickness ratios, gradient index and the transverse shear on buckling temperature difference are all studied.

2. Material properties of S-FGM plates

Consider a rectangular plate made of a mixture of metal and ceramic as shown in Figure 1.

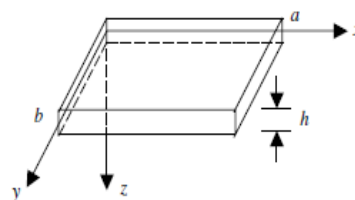


Fig 1 .Configuration and coordinate system of a rectangular plate.

In the case of adding an FGM of a single power-law function to the multi-layered composite, stress concentrations appear on one of the interfaces where the material is continuous but changes rapidly [21, 22]. Therefore, Chung and Chi [19] and Sallai et al. [1] defined the volume fraction using two power-law functions to ensure smooth distribution of stresses among all the interfaces. The two power-law functions are defined by:

$$V_1(z) = 1 - \frac{1}{2} \left(1 - \frac{2z}{h}\right)^k \text{ for } 0 \leq z \leq h/2 \quad (1a)$$

$$V_2(z) = \frac{1}{2} \left(1 + \frac{2z}{h}\right)^k \text{ for } -h/2 \leq z \leq 0 \quad (1b)$$

Where k is the material gradient index.

By using the rule of mixture, the Young's modulus E and the coefficient of thermal expansion α of the S-FGM can be calculated by:

$$E(z) = E_m + V_1(z)E_{cm} \text{ for } 0 \leq z \leq h/2 \quad (2a)$$

$$E(z) = E_m + V_2(z)E_{cm} \text{ for } -h/2 \leq z \leq 0 \quad (2b)$$

$$\alpha(z) = \alpha_m + V_1(z)\alpha_{cm} \text{ for } 0 \leq z \leq h/2 \quad (2c)$$

$$\alpha(z) = \alpha_m + V_2(z)\alpha_{cm} \text{ for } -h/2 \leq z \leq 0 \quad (2d)$$

Where E_m and α_m denote the elastic moduli and the coefficient of thermal expansion of metal respectively; E_c and α_c denote the elastic moduli and the coefficient of thermal expansion of ceramic respectively. We note that: $E_{cm} = E_c - E_m$ and $\alpha_{cm} = \alpha_c - \alpha_m$

Figure 2 shows the volume fraction distribution of ceramic phase through the thickness for several values of the power law index. The variation of the composition of ceramics and metal is linear for $k = 1$. The volume fraction rapidly changes near the top and bottom surfaces for $k < 1$ but vary quickly near the middle surface for $k > 1$. Therefore, if the S-FGM plate is used as the undercoat in a laminated material, the material distribution with $k > 1$ is the better choice.

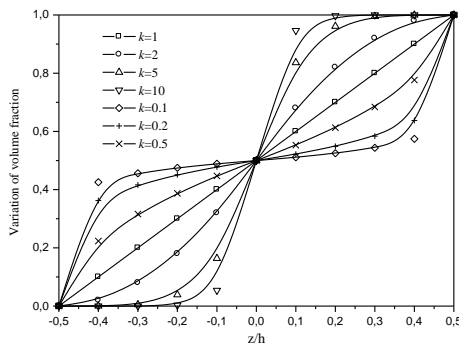


Fig 2. Variation of the volume fraction through the thickness of an S-FGM plate with differing material gradient index k .

3. Analysis

The S-FGM plate is assumed simply supported in bending and rigidly fixed in extension. The temperature change is varied only in the thickness direction. Assume that u, v, w denote the displacements of the neutral plane of the plate in x, y, z directions respectively; ϕ_x, ϕ_y denote the rotations of the normals to the plate midplane. According to the first order shear deformation theory, the strains of the plate can be expressed as

$$\begin{aligned} \epsilon_x &= u_{,x} + z\phi_{x,x} & \epsilon_y &= v_{,y} + z\phi_{y,y} \\ \gamma_{xy} &= u_{,y} + v_{,x} + z(\phi_{x,y} + \phi_{y,x}) \\ \gamma_{xz} &= \phi_x + w_{,x} & \gamma_{zy} &= \phi_y + w_{,y} \end{aligned} \quad (3)$$

Hooke's law for a plate is defined as

$$\begin{aligned} \sigma_x &= \frac{E}{1-\nu^2} (\epsilon_x + \nu\epsilon_y - (1+\nu)\alpha T) \\ \sigma_y &= \frac{E}{1-\nu^2} (\epsilon_y + \nu\epsilon_x - (1+\nu)\alpha T) \\ \tau_{xy} &= \frac{E}{2(1+\nu)} \gamma_{xy}, \quad \tau_{zx} = \frac{E}{2(1+\nu)} \gamma_{zx} \\ \tau_{zy} &= \frac{E}{2(1+\nu)} \gamma_{zy} \end{aligned} \quad (4)$$

The forces and moments per unit length of the plate expressed in terms of the stress components through the thickness are

$$\begin{Bmatrix} N_x \\ N_y \\ N_{xy} \end{Bmatrix} = \int_{-h/2}^{h/2} \begin{Bmatrix} \sigma_x \\ \sigma_y \\ \tau_{xy} \end{Bmatrix} dz, \quad \begin{Bmatrix} M_x \\ M_y \\ M_{xy} \end{Bmatrix} = \int_{-h/2}^{h/2} \begin{Bmatrix} \sigma_x \\ \sigma_y \\ \tau_{xy} \end{Bmatrix} z dz, \quad \begin{Bmatrix} Q_{xy} \\ Q_{yx} \end{Bmatrix} = \int_{-h/2}^{h/2} \begin{Bmatrix} \tau_{xy} \\ \tau_{yx} \end{Bmatrix} dz \quad (5)$$

Substituting Eqs. (2), (3), and (4) into Eqs. (5), gives the constitutive relations as

$$\begin{aligned} N_x &= \frac{E_1}{1-\nu^2} (u_{,x} + \nu v_{,y}) + \frac{E_2}{1-\nu^2} (\phi_{x,x} + \nu \phi_{y,y}) - \frac{\Phi}{1-\nu} \\ N_y &= \frac{E_1}{1-\nu^2} (\nu u_{,x} + v_{,y}) + \frac{E_2}{1-\nu^2} (\nu \phi_{x,x} + \phi_{y,y}) - \frac{\Phi}{1-\nu} \\ N_{xy} &= \frac{E_1}{2(1+\nu)} (u_{,y} + v_{,x}) + \frac{E_2}{2(1+\nu)} (\phi_{x,y} + \phi_{y,x}) \\ M_x &= \frac{E_2}{1-\nu^2} (u_{,x} + \nu v_{,y}) + \frac{E_3}{1-\nu^2} (\phi_{x,x} + \nu \phi_{y,y}) - \frac{\Theta}{1-\nu} \\ M_y &= \frac{E_2}{1-\nu^2} (\nu u_{,x} + v_{,y}) + \frac{E_3}{1-\nu^2} (\nu \phi_{x,x} + \phi_{y,y}) - \frac{\Theta}{1-\nu} \\ M_{xy} &= \frac{E_2}{2(1+\nu)} (u_{,y} + v_{,x}) + \frac{E_3}{2(1+\nu)} (\phi_{x,y} + \nu \phi_{y,x}) \\ Q_x &= \frac{E_1}{2(1+\nu)} (\phi_x + w_{,x}) \\ Q_y &= \frac{E_1}{2(1+\nu)} (\phi_y + w_{,y}) \end{aligned} \quad (6)$$

Where

$$(E_1, E_2, E_3) = \int_{-h/2}^{h/2} (1, z, z^2) E(z) dz, \quad (7)$$

$$(\Phi, \Theta) = \int_{-h/2}^{h/2} E(z) \alpha(z) T(x, y, z) (1, z) dz$$

The nonlinear equations of equilibrium according to Von Karman's theory are given by

$$\begin{aligned} N_{x,x} + N_{xy,y} &= 0 \\ N_{y,y} + N_{xy,x} &= 0 \\ M_{x,x} + M_{xy,y} - Q_x &= 0 \\ M_{xy,x} + M_{y,y} - Q_y &= 0 \\ Q_{x,x} + Q_{y,y} + N_x w_{,xx} + N_y w_{,yy} + 2N_{xy} w_{,xy} &= 0 \end{aligned} \quad (8)$$

Using Eqs. (6) and (8) and by eliminating the variables u, v, ϕ_x, ϕ_y , the equations of equilibrium can be covered into one equation as

$$\begin{aligned} \nabla^4 w + \frac{2(1+\nu)}{E_1} \nabla^2 (N_x w_{,xx} + N_y w_{,yy} + 2N_{xy} w_{,xy}) \\ - \frac{E_1(1-\nu^2)}{E_1 E_3 - E_2^2} (N_x w_{,xx} + N_y w_{,yy} + 2N_{xy} w_{,xy}) = 0 \end{aligned} \quad (9)$$

To establish the stability equations, the critical equilibrium method is used. Assuming that the state of stable equilibrium of a general plate under thermal load may be designated by w_0 . The displacement of the neighboring state is $w_0 + w_1$, where w_1 is an arbitrarily small increment of displacement. Substituting $w_0 + w_1$ into Eq. (9) and subtracting the original equation, results in the following stability equation

$$\begin{aligned} \nabla^4 w_1 + \frac{2(1+\nu)}{E_1} \nabla^2 (N_x^0 w_{1,xx} + N_y^0 w_{1,yy} + 2N_{xy}^0 w_{1,xy}) \\ - \frac{E_1(1-\nu^2)}{E_1 E_3 - E_2^2} (N_x^0 w_{1,xx} + N_y^0 w_{1,yy} + 2N_{xy}^0 w_{1,xy}) = 0 \end{aligned} \quad (10)$$

Where, N_x^0, N_y^0 and N_{xy}^0 refer to the pre-buckling force resultants.

3.1. Buckling of S-FGM plates under uniform temperature rise

To determine the buckling temperature difference ΔT_{cr} , the pre-buckling thermal forces should be found firstly. Solving the membrane form of equilibrium equations, gives the pre-buckling force resultants

$$N_x^0 = -\frac{\Phi}{1-\nu}, N_y^0 = -\frac{\Phi}{1-\nu}, N_{xy}^0 = 0 \quad (11)$$

Substituting Eq. (11) into Eq. (10), one obtains

$$\begin{aligned} \nabla^4 w_1 - \frac{2(1+\nu)}{E_1} \frac{\Phi}{1-\nu} \nabla^4 w_1 \\ + \frac{E_1(1-\nu^2)}{E_1 E_3 - E_2^2} \frac{\Phi}{1-\nu} \nabla^2 w_1 = 0 \end{aligned} \quad (12)$$

If the transverse shear deformation is not considered, Eq. (12) can be reduced as

$$\nabla^4 w_1 + \frac{E_1(1-\nu^2)}{E_1 E_3 - E_2^2} \frac{\Phi}{1-\nu} \nabla^2 w_1 = 0 \quad (13)$$

The simply supported boundary condition is defined as

$$\begin{aligned} w_1 = 0, M_{x1} = 0, \phi_{y1} = 0 \text{ on } x = 0, a \\ w_1 = 0, M_{y1} = 0, \phi_{x1} = 0 \text{ on } y = 0, b \end{aligned} \quad (14)$$

The following approximate solution is seen to satisfy both the governing equation and the boundary conditions

$$w_1 = c \sin(m\pi x/a) \sin(n\pi y/b) \quad (15)$$

Where m, n are number of half waves in the x and y directions, respectively, and c is a constant coefficient.

Substituting Eq. (15) into Eq. (13), and substituting for the thermal parameter Φ from Eq. (7), yields

$$\Delta T = \frac{(E_1 E_3 - E_2^2)(1-\nu)\pi^2(m^2 + n^2 B_a^2)}{2(1+\nu)(E_1 E_3 - E_2^2)\pi^2(m^2 + n^2 B_a^2) + E_1^2 a^2(1-\nu^2)} \frac{E_1}{P} \quad (16)$$

Where

$$P = E_m \alpha_m h + \frac{(E_{cm} \alpha_m + E_m \alpha_{cm})h}{k+1} + \frac{E_{cm} \alpha_{cm} h}{2k+1} \quad (17)$$

and $B_a = a/b$

The critical temperature difference is obtained for the values of m, n that make the preceding expression a minimum. Apparently, when minimization methods are used, critical temperature difference is obtained for the fundamental mode $m = n = 1$ [5-6-8], thus

$$\Delta T_{cr} = \frac{(E_1 E_3 - E_2^2)(1-\nu)\pi^2(1+B_a^2)}{2(1+\nu)(E_1 E_3 - E_2^2)\pi^2(1+B_a^2) + E_1^2 a^2(1-\nu^2)} \frac{E_1}{P} \quad (18)$$

3.2. Buckling of S-FGM plates under sinusoidal temperature change

The temperature rise under sinusoidal temperature distribution across the thickness is assumed as

$$T(z) = \Delta T [1 - \cos(\frac{\pi z}{2h} + \frac{\pi}{4})] + T_m \quad (19)$$

For this loading case, the thermal parameter Φ can be expressed as

$$\Phi = P(T_m + \Delta T) - Y\Delta T \quad (20)$$

Where

$$Y = \int_{-h/2}^{h/2} E(z)\alpha(z) \cos\left(\frac{\pi z}{2h} + \frac{\pi}{4}\right) dz \quad (21)$$

From Eq.(20) one has

$$\Delta T = \frac{\Phi - PT_m}{P - Y} \quad (22)$$

When the approximate solution (15) is substituted into Eq. (12), and the definition of parameter Φ from Eq. (7) are used, the expression for thermal buckling of the plate is obtained. Taking $m = n = 1$, the critical buckling temperature is expressed as

$$\Delta T_{cr} = \left(\frac{(E_1 E_3 - E_2^2)(1-\nu)\pi^2(1+B_a^2)E_1}{2(1+\nu)(E_1 E_3 - E_2^2)\pi^2(1+B_a^2) + E_1^2 a^2(1-\nu^2)} - PT_m \right) \frac{1}{P - Y} \quad (23)$$

4. Results and discussion

The thermal buckling analysis is conducted for combinations of metal and ceramic. The set of materials chosen is Aluminum and Alumina. For simplicity, Poisson's ratio of the two materials is assigned the same value. Typical values for metal and ceramics used in the S-FGM plate are listed in Table 1.

Table1
Material properties used in the S-FGM plate

Properties	Metal: Al	Ceramic: Al ₂ O ₃
E (GPa)	70	380
ν	0.3	0.3
α ($10^{-6}/^\circ\text{C}$)	23	7.4

Firstly, the critical temperature differences are calculated for sigmoid functionally graded plates under uniform temperature and sinusoidal temperature change, respectively. The obtained results are plotted in Figure 3 and they show the critical buckling temperature difference ΔT_{cr} vs. the thickness to span ratio h/a where the material gradient index k is equal to 2 and $a/b = 1$. It is seen that the critical temperature difference increases monotonically as the relative thickness h/a increases. The values of the critical temperature differences calculated by using the first order shear deformation theory are lower than those calculated by using the classical plate theory.

This means that the inclusion of effect of transverse shear deformation leads to a reduction in the critical buckling temperature difference, especially for thick plates.

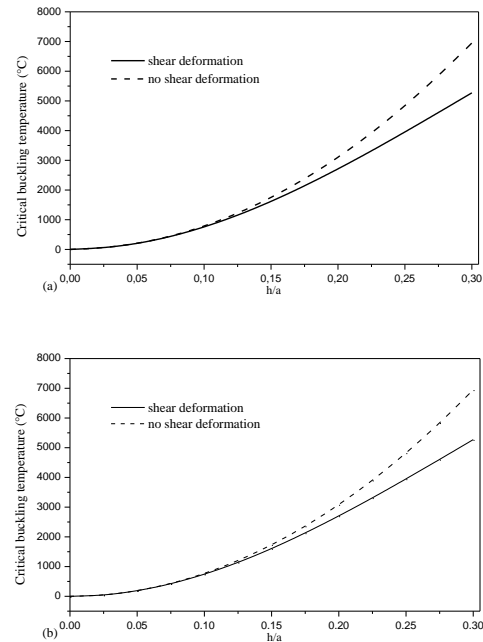


Fig3. Critical buckling temperature of S-FGM plate vs. relative thickness of the plate: (a) under uniform temperature change; (b) under sinusoidal temperature change.

Figure 4 shows the effect of temperature change on the variation trend of critical temperature difference with respect to the plate aspect ratio a/b for the material gradient index k equal to 2. The relative thickness of the plate is set as $h/a = 0.2$. It is observed that with increasing the plate aspect ratio a/b from 1 to 10, the critical buckling temperature difference also increases steadily. From Figure 6 It is found that the values of the buckling temperature difference computed with sinusoidal temperature distribution across the thickness are higher than those computed by linear temperature distribution.

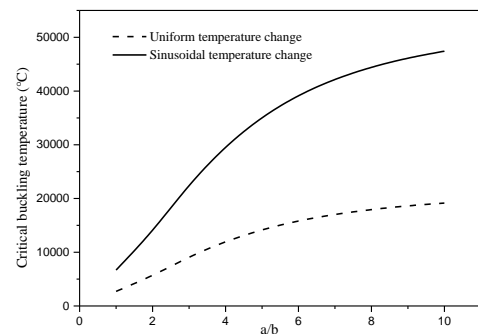


Fig 4. Effect of the temperature change on critical buckling temperature of S-FGM plate ($h/a = 0.2$ and $k = 2$).

Figure 5 shows the buckling temperature vs. the material gradient index k for a plate with $h/a=0.2$ and $a=b$. We can see that the critical buckling temperature for a homogeneous plate with $k=0$ is considerably higher than those for the sigmoid functionally graded plate with $k>0$. It is evident that the critical buckling temperature difference decreases as the material gradient index k increases monotonically. However, it can be seen that for sinusoidal temperature distribution assumption across the thickness, the critical buckling temperature difference increases for the lower values of the material gradient index $0 < k < 0.5$.

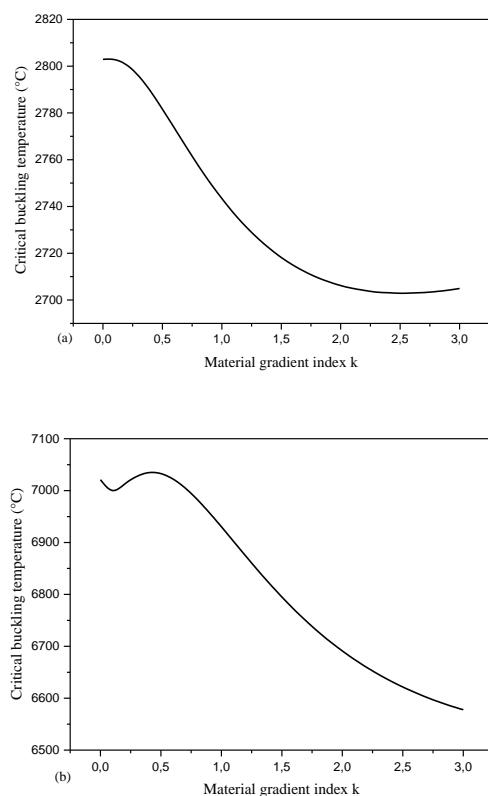


Fig 5. Critical buckling temperature rise of an S-FGM plate vs. material gradient index k : (a) uniform temperature change; (b) sinusoidal temperature change;

5. Conclusions

Critical buckling temperatures of simply supported homogeneous and inhomogeneous composite plates have been analyzed by using the first shear deformation plate theory. The inhomogeneous plates are considered as Al/Al₂O₃ S-FGM plates. The buckling analysis of such a plate under two types of thermal loadings is investigated. It is shown that both the transverse shear deformation and the material gradient index have considerable effect on the critical buckling temperature difference of S-FGM plate, especially for a thick plate or a plate with large aspect ratio.

References

- [1] B.O. Sallai, A. Tounsi, I. Mechab, M. Bachir Bouiadjra, M. Meradjah, E.A. Adda Bedia "A theoretical analysis of flexional bending of Al/Al₂O₃ S-FGM thick beams" *Computational Materials Science* 44 (2009) 1344–1350.
- [2] S. Merdaci, A. Tounsi, M.S.A. Houari, I. Mechab, H. Hebali, S. Benyoucef "Two new refined shear displacement models for functionally graded sandwich plates" *Archive of Applied Mechanics*, (In press) 2011.
- [3] Mechab I., Ait Atmane H., Tounsi A., Belhadj H. A., Adda bedia E.A. "A two variable refined plate theory for bending of functionally graded plates," *Acta Mech Sin*, 26(6): 941, 2010.
- [4] Houari M.S.A, Benyoucef S., Mechab I., Tounsi A., Adda bedia E.A. "Two variable refined plate theory for thermoelastic bending analysis of functionally graded sandwich plates," *J. Thermal Stresses*, (Accepted), 2010.
- [5] N. El Meiche, A. Tounsi, N. Ziane, I. Mechab, E.A. Adda Bedia "A new hyperbolic shear deformation theory for buckling and vibration of functionally graded sandwich plate" *International Journal of Mechanical Sciences* (In press) 2011.
- [6] Javaheri R, Eslami MR. Thermal buckling of functionally graded plates. *AIAA J* 2002; 40:162–9.
- [7] Lanhe Wu. Thermal buckling of a simply supported moderately thick rectangular FGM plate. *Compos Struct* 2004; 64:211–8.
- [8] Najafizadeh MM, Eslami MR. First-order-theory-based thermoelastic stability of functionally graded circular plates. *AIAA J* 2002; 40:1444–50.
- [9] Z.H. Jin, G.H. Paulino, "Transient thermal stress analysis of an edge crack in a functionally graded material" *International Journal of Fracture* 107 (2001) 73–98.
- [10] Y.Y. Yung, D. Munz, in: T. Shiota, M.Y. Miyamoto (Eds.), *Functionally Graded Material*, 1996, pp. 41–46.
- [11] Zhang Da-Guang, Zhou You-He, "A theoretical analysis of FGM thin plates based on physical neutral surface" *Computational Materials Science* 44 (2008) 716 – 720.
- [12] S. Joshi, A. Mukherjee, S. Schmauder, "Exact solutions for characterization of electro-elastically graded materials" *Computational Materials Science* 28 (2003) 548–555.
- [13] Z.H. Jin, R.C. Batra, "Stresses intensity relaxation at the tip of an edge crack in a functionally graded material subjected to a thermal shock" *Journal of Thermal Stresses* 19 (1996) 317–339.
- [14] F. Delale, F. Erdogan, "The crack problem for a nonhomogeneous plane" *ASME Journal of Applied Mechanics* 50 (1983) 609–614.
- [15] P. Gu, R.J. Asaro, "Crack deflection in functionally graded materials" *International Journal of Solids and Structures* 34 (1997) 3085–3098.
- [16] F. Erdogan, B.H. Wu, "Crack problems in FGM layers under thermal stresses" *Journal of Thermal Stresses* 19 (1996) 237–265.
- [17] Z.H. Jin, N. Noda, "Crack tip singular fields in nonhomogeneous materials" *ASME Journal of Applied Mechanics* 61 (1994) 738–740.
- [18] F. Erdogan, Y.F. Chen, "Interfacial cracking of FGM/metal bonds" in: K. Kokini (Ed.), *Ceramic Coating*, 1998, pp. 29–37.
- [19] Y.L. Chung, S.H. Chi, "The residual stress of functionally graded materials" *Journal of the Chinese Institute of Civil and Hydraulic Engineering* 13 (2001) 1–9.
- [20] S.H. Chi, Y.L. Chung, "Cracking in sigmoid functionally graded coating" *Journal of Mechanics* 18 (2002) 41–53.
- [21] Y.D. Lee, F. Erdogan, "Residual/thermal stresses in FGM and laminated thermal barrier coatings" *International Journal of Fracture* 69 (1995), 145 –165.
- [22] G. Bao, L. Wang, "Multiple cracking in functionally graded ceramic/metal coatings" *International Journal of Solids and Structure* 32 (1995), 2853 –2871.